Polyhedron 30 (2011) 1671–1679

Contents lists available at ScienceDirect

Polyhedron

journal homepage: www.elsevier.com/locate/poly

Synthesis, chemical characterization and preliminary *in vitro* antitumor activity evaluation of new ruthenium(II) complexes with sugar derivatives

Gianfranco Fontana [a], Michele Abbate [b,*], Girolamo Casella [b], Claudia Pellerito [b], Alessandro Longo [c], Francesco Ferrante [b]

[a] Dipartimento di Scienze e Tecnologie Molecolari e Biomolecolari (STEMBIO), Università degli Studi di Palermo, Viale delle Scienze, Parco d'Orleans II, Ed. 17, 90128 Palermo, Italy
[b] Dipartimento di Chimica "Stanislao Cannizzaro", Università degli Studi di Palermo, Viale delle Scienze, Parco d'Orleans II, Ed. 17, 90128 Palermo, Italy
[c] C.N.R. – I.S.M.N. via Ugo La Malfa 153, 90146 Palermo, Italy

ARTICLE INFO

Article history:
Received 5 May 2010
Accepted 23 March 2011
Available online 14 April 2011

Keywords:
Ruthenium(II)
Carbohydrates
Anti-cancer
Melanoma A375

ABSTRACT

Three new complexes of Ru(II), namely $[RuCl_2(Glun\text{-}N,O)_2]Na_2$ (**I**; Glun = glucosaminate), $[RuCl_2(1\text{-}Tglu)(EtOH)_2]Na$ (**II**; 1-Tglu = 1-thio-β-D-glucose) and $[Ru_2(EtOH)_6(AL)Cl_4]$ (**III**; AL = 6′-aminolactose) were prepared from the same Ru(II) precursor, $[RuCl_2(DMSO)_4]$ (DMSO = dimethyl sulfoxide). The characterization of the complexes was carried out by elemental analysis, FT-IR, ES-MS, NMR, EXAFS and DFT calculations. The effectiveness of the complexes on metastatic melanoma A 375 was investigated. The results show that complex **II** is the most active species.

1. Introduction

Ruthenium complexes are increasingly attracting the interest of researchers due to their promising pharmacological properties [1a,b]. Particularly with ligands of biological relevance, the preferred octahedral coordination for the common (II) and (III) oxidation states in aqueous solution, together with adequate substitution rates and redox potentials for biological interactions and a demonstrated low toxicity make ruthenium a particularly attractive choice for the development of new metallopharmaceuticals [2–11].

The first representative of bioactive ruthenium complexes is the Ru(III) complex *trans*-$[RuCl_4(Im)(DMSO)][ImH]$ (NAMI-A; Im = imidazole), synthesized and characterized by Sava et al. in Trieste, which possesses outstanding antimetastatic activity [12] and it has completed phase I clinical trials [13]. Further, *trans*-$[RuCl_4(Ind)_2][IndH]$ (KP1019; Ind = indazole) [14–16] possesses a high activity against colon cancer [17]. The effectiveness of NAMI-A on the metastatic melanoma B16 has recently been demonstrated and it was suggested that the metastasis inhibition is due to the negative modulation of tumor cell invasion processes, a mechanism in which the reduction of the gelatinolytic activity of tumor cells plays a crucial role [18].

Some interesting examples of bioactive Ru(II) complexes are Ru(II)–arene/ethylenediamine and related derivatives as well as Ru(II)–arene–PTA complexes (PTA = 1,3,5-triaza-7-phosphaadamantane) [19]. Further, *cis*- and *trans*-$[RuCl_2(DMSO)_4]$, two neutral octahedral Ru(II) compounds, showed significant antitumor activity [20–22]. The *trans* isomer is markedly more toxic and reactive than the *cis* one [21,23].

The aim of this work was to prepare three new Ru(II) complexes with carbohydrate-based ligands and to investigate their cytotoxicity *in vitro* on melanoma A375 cell lines. This biological target was chosen considering that A375 cells are relatively resistant to many standard cancer therapies [24–26] and the Ru(II)-derived complex $[Ru(bbdo)(dppz)](ClO_4)_2$ (bbdo = 1,8-bis(benzimidazol-2-yl)-3,6-dithiaoctane, dppz = dipyrido[3,2a:2′,3′-c]phenazine) showed selective inhibition activity against this cell line [27]. The structures of the ligands employed are reported in Fig. 1. To the best of our knowledge, little of work has been done to investigate carbohydrate based ruthenium complexes [28], though the use of these ligands may imply potentially interesting consequences for the metabolism, bioavailability and administration procedure of the drugs [1b].

2. Experimental

2.1. Materials

All the reagents used were chemically pure or analytical reagent grade. Ethanol was from J.T. Beaker (Italy). D-Glucosaminic acid

* Corresponding author. Tel.: +39 91 590367; fax: +39 91 427584.
E-mail addresses: fontgian@unipa.it (G. Fontana), micheleabbate@unipa.it (M. Abbate), gcasella@unipa.it (G. Casella), bioinorg@unipa.it (C. Pellerito), alex@pa.ismn.cnr.it (A. Longo), f.ferrante@unipa.it (F. Ferrante).

0277-5387/$ - see front matter © 2011 Elsevier Ltd. All rights reserved.
doi:10.1016/j.poly.2011.03.046

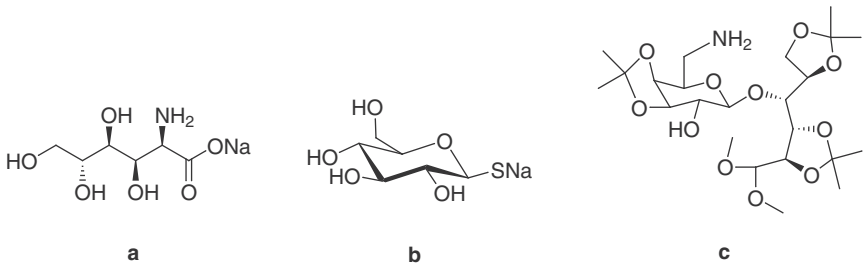

Fig. 1. Chemical structures of D-glucosaminic acid sodium salt (a), 1-thio-β-D-glucose sodium salt (b) and 6′-aminolactose precursor (c).

was from Fluka (Italy) and the 1-thio-β-D-glucose sodium salt was from Aldrich (Italy).

The starting complex, $[RuCl_2(DMSO)_4]$, was prepared by reported literature methods [20–22]. Glucosaminic acid was deprotonated according to the following procedure: 390 mg (2 mmol) of the acid were dissolved in 5 mL of ethanol, then NaOH (120 mg, 3 mmol) was added in one portion. The solution was stirred for 30 min, then the solvent removed by rotary evaporation. The residual water was removed by several co-evaporation steps with toluene.

2.2. Physical measurements

2.2.1. Elemental analysis

The recrystallized solids were analyzed for C, H, N and S, using a Vario EL III CHNS elemental analyzer (Elementar Analysensysteme GmbH, Hanau, Germany) in our laboratory. Chlorine was determined by the Schöniger W. method [29].

2.2.2. FT-IR spectroscopy

FT-IR spectra were registered, as KBr pellets or in Nujol mulls in CsI windows, on a Mod. Spectrum One Perkin–Elmer FT-IR spectrophotometer, in the 4000–300 cm^{-1} region.

2.2.3. Mass spectroscopy

Electrospray ionization (ESI) MS spectra were recorded on a Finnigan LCQ-Duo ion trap electrospray mass spectrometer (Bremen, Germany). Sample solutions were introduced into the ESI source via 100 μm i.d. fused silica, from a 250 μL syringe. The experimental conditions for the spectra, acquired in positive ion mode, were as follows: needle voltage 5 kV; flow rate 5 μL/min; source temperature 150 °C; m/z range 200–2000; cone potential 46 V; tube lens offset 15 V.

High-resolution (HR) MS were recorded using an Autospec Ultima o-TOF (Micromass, Manchester, UK) mass spectrometer connected with a gas chromatography (GC) system HP 6890 series (Hewlett Packard, Palo Alto, CA, USA).

2.2.4. NMR spectroscopy

One-dimensional ^1H, $^{13}C\{^1H\}$ and two-dimensional ^1H-COSY, (^1H–^{13}C)-gHSQC, (^1H–^{13}C)-gHMBC spectra were acquired at 298 K on a Bruker ARX 300 (7.04 T) spectrometer at 300.13 and 76.45 MHz with spectral widths corresponding to windows of 10 and 200 ppm, respectively. The ^1H and $^{13}C\{^1H\}$ spectra of the free ligands were acquired in $CDCl_3$ and calibrated by the solvent's proton and carbon resonances (^1H, δ = 7.26 ppm; ^{13}C, δ = 77.16 ppm). For compounds **I** and **II**, the ^1H NMR spectra were acquired in D_2O and D_2O/EtOH-d6 (1:1 V/V) solutions, respectively, and the external reference for ^1H and ^{13}C were the resonances of 4,4-dimethyl 4-silapentane sodium sulfonate (DSS) (^1H, δ = 0.00 ppm; ^{13}C, δ = 0.00 ppm). For compound **III**, the ^1H NMR spectrum was acquired in DMSO-d6 solution and calibrated upon the solvent's proton and carbon resonances (^1H, δ = 2.51 ppm; ^{13}C, δ = 39.52 ppm). $^{13}C\{^1H\}$ spectra were acquired with broadband proton powergated decoupling. The concentrations for all the samples were in the 0.05–0.10 M range.

2.2.5. Optical rotations

Optical rotations were recorded on a Jasco P-1010 polarimeter. The specific rotation was obtained in $CHCl_3$ at 29 °C.

2.2.6. Flash chromatography (FC): Si gel Merck LiChroprep® 15–25/25–40 μm 1/1 was used for flash chromatography (elution under 0.7 psi of Ar)

2.2.6.1. EXAFS spectroscopy. EXAFS spectra were recorded in the transmission mode at beam line XAFS at the ELETTRA synchrotron (Trieste, Italy). Spectra at the Ru K-edge at 22.117 eV were acquired at low temperature (80 K) using a Si(1 1 1) monochromator. For Ru K-edge measurements a ruthenium metal foil was used as a reference. Detection was performed by using three ionization chambers, reading the intensity before and after the sample and after the reference sample, respectively. The energy was calibrated to the first inflection point of the Ru-metal foil. A total of 2–4 scans were collected for each sample for an analysis time of about 1 h in order to get an acceptable signal-to-noise ratio. Extraction and fitting of the EXAFS signal were performed by standard procedures using the HORAE software suite [30]. Fourier transforms (FT) of the $w(k)k^2\chi$ (k) EXAFS data were carried out in the range 2–12 $Å^{-1}$. The phase shift and backscattering amplitude factor were corrected by using the calculated values of FEFF6 [31], for Ru as an absorber and Cl, S, O and N as scatterers.

2.2.7. Computational details

Density functional calculations have been performed with GAUSSIAN 03 [32] on a number of isomers of complexes **I**–**III** using the B3LYP functional [33] (in restricted and unrestricted forms) joined with the correlation consistent polarized valence double zeta, cc-pVDZ, basis set for light atoms and the Relativistic Small Core Stuttgart '97 Effective Core Potential for ruthenium, with the corresponding valence basis set. Various spin multiplicities have been investigated for the three ruthenium complexes, and the singlet state was always the most stable. The character of the minimum in the potential energy surface of all the optimized geometries has been checked by inspection of the harmonic vibrational frequencies; accordingly all energy values here reported have been corrected for the zero point vibrational contribution.

2.3. Synthesis

2.3.1. Synthesis of the ligand **c**

2.3.1.1. 6′-Phtalimido-2,3:5,6:3′,4′-tri-O-isopropylidenelactose dimethyl acetal (c″, Scheme 1). About 280 μL (288 mg, 1.35 mmol) of diisopropyl azodicarboxylate were added dropwise to a stirred solution of 200 mg (0.393 mmol) of compound **c′**, 360 mg (1.37 mmol) of triphenylphosphine and 200 mg (1.36 mmol) of phtalimide at 0 °C under Ar. Then the solution was warmed to

room temperature (RT) and stirred overnight. The solvent was removed under reduced pressure and the residue was partitioned between brine and ethyl acetate. The organic phase was washed with water and dried over Na_2SO_4. The solvent was removed by a rotary evaporator and the residue was purified by flash chromatography (FC) (elution with EtOAc–petroleum ether in gradient from 3:7 to 7:3) to give pure **c**″.

Compound **c**″: amorphous solid; yield: 55.0%; $[\alpha]_D^{29}$ + 8.9 (c 0.336, $CHCl_3$); IR (KBr) ν_{max} cm^{-1}: 3428, 3029, 2990, 1718, 1216, 1071, 1103. ^1H NMR (300 MHz, $CDCl_3$) δ galacto moiety: 3.80 (dd, $J_{6A'-6B'}$ = 14.0, $J_{6A'-5'}$ = 10.3, 1H, H-6′A), 4.06 (m, 1H, H-4′), 4.08 (dd, $J_{2'-1'} = J_{2'-3'}$ = 7.8, 1H, H-2′), 4.11 (m, 1H, H-3′), 4.12 (m, 1H, H-5′), 4.18 (dd, $J_{6'B-6'A}$ = 10.3, $J_{6'B-5'}$ = 5.3, 1H, H-6′B), 4.21 (d, $J_{1'-2'}$ = 8.0, 1H, H-1′); gluco moiety: 3.53 (m, 1H, H-5), 3.73 (m, 1H, H-2), 3.90 (m, 1H, H-6A), 3.92 (d, J_{1-2} = 4.3, 1H, H-1), 3.97 (m, 2H, H-6B + H-4), 4.00 (m, 1H, H-3); other signals: 1.27 (s, 6H, 2 × CH_3 isopropylidene), 1.31 (s, 3H, CH_3 isopropylidene), 1.34 (s, 3H, CH_3 isopropylidene), 1.47 (s, 3H, CH_3 isopropylidene), 1.57 (s, 3H, CH_3 isopropylidene), 3.22 (s, 3H, OCH_3), 3.31 (s, 3H, OCH_3), 7.47–8 (m, 4H, CH aryl). ^{13}C NMR (75.00 MHz, $CDCl_3$) δ galacto moiety: 39.2 (t, C-6′), 71.00 (d, C-5′), 73.5 (d, C-3′), 75.5 (d, C-2′), 77.9 (d, C-3′), 104.4 (d, C-1′); gluco moiety: 65.0 (t, C-6), 74.4 (d, C-5), 77.1 (d, C-2), 77.5 (d, C-4), 79.1 (d, C-3), 104.8 (d, C-1); other signals: 25.2–28.5 (6 peaks, q, C(CH_3)$_2$), 54.4 (q, OMe), 57.5 (q, OMe), 108.5 (s, $C(CH_3)_2$), 110.0 (s, $C(CH_3)_2$), 110.7 (s, $C(CH_3)_2$), 123.8 (d, aromatic C), 131.5 (s, aromatic C), 134.3 (d, aromatic C), 168.5 (s, imidic carbonyl). HRMS: *m*/*z* 637.6717, calculated for $C_{31}H_{43}NO_{13}$: 637.2734.

2.3.1.2. 6′-Amino-2,3:5,6:3′,4′-tri-O-isopropylidenelactose dimethyl acetal (c, Scheme 1). To a solution of 640 mg (1 mmol) of compound **c**″ in 2 mL of absolute EtOH, 11 μL of monohydrate hydrazine were added in one portion. The resulting solution was refluxed for 3.5 h and then slowly cooled to 0 °C and kept at this temperature for 12 h. A precipitate appeared that was filtered off. The solution was reduced to a small volume by rotary distillation and treated with 1:1 HCl until a pH value of 4 was reached. Then 10 mL of brine were added to the solution, which was then extracted with 2:1 $CHCl_3$/EtOH. The solvent was removed by rotary distillation and the residue, still containing large amount of "phthalate derivate" impurities was suspended in 2:1 EtOH/H_2O and treated with 1 N NaOH until a pH value of 12 was obtained, and then it was stirred for 1 h. Afterward the solvent was removed by rotary distillation and the residual slurry was crushed and stirred into 10 mL of ethyl acetate. Finally the organic phase was passed through a funnel containing a short pad of Celite under a pad of dry Na_2SO_4 between two layers of sea sand. The subsequent purification by FC (light petroleum/EtOAc 1:1, then pure EtOAc, then EtOAc/MeOH 8:2) afforded compound **c**, see Fig. 1 (67% yield).

Compound **c**: caramel colored amorphous solid; $[\alpha]_D^{29}$ + 29.8 (c 0.420, $CHCl_3$); IR (KBr) ν_{max} cm^{-1}: 3365, 3304, 3184, 1253, 1216, 1075; ^1H NMR (300 MHz, $CDCl_3$) δ galacto moiety: 2.86 (dd, $J_{6'A-6'B}$ = 13.3, $J_{6'A-5'}$ = 2.0, 1H, H-6′A), 3.06 (dd, $J_{6'B-6'A}$ = 13.3, $J_{6'B-5'}$ = 9.6, 1H, H-6′B), 3.45 (m, 1H, H-2′), 3.66 (m, 1H, H-5′), 3.99 (m, 1H, H-3′), 4.25 (m, 1H, H-4′), 4.37 (d, $J_{1'-2'}$ = 8.2, 1H, H-1′); gluco moiety 3.84 (m, 1H, H-3), 3.95 (m, 1H, H-6A), 3.98 (m, 1H, H-5), 4.00 (m, 1H, H-4), 4.13 (dd, J_{6B-6A} = 8.0, J_{6B-5} = 6.0, 1H, H-6B), 4.28 (d, J_{1-2} = 6.0, 1H, H-1), 4.45 (dd, $J_{2-1} = J_{2-3}$ = 6.9, 1H, H-2); other signals: 1.25 (s, 6H, 2 × CH_3 isopropylidene), 1.32 (s, 6H, 2 × CH_3 isopropylidene), 1.43 (s, 6H, 2 × CH_3 isopropylidene), 3.92 (s, 3H, OCH_3), 3.41 (s, 3H, OCH_3).

^{13}C NMR (75.00 MHz, $CDCl_3$) δ galacto moiety: 43.0 (t, C-6′), 74.5 (d, C-2′), 74.9 (d, C-5′), 78.2 (d, C-4′), 79.6 (d, C-3′), 103.8 (d, C-1′); gluco moiety 64.8 (t, C-6), 75.2 (d, C-4), 76.1 (d, C-5), 76.2 (d, C-2), 78.5 (d, C-3), 107.1 (d, C-1); other signals 24.9–29.1 (q, 6 peaks, C(CH_3)$_2$), 54.1 (q, OCH_3), 56.5 (q, OCH_3), 107.7 (s, $C(CH_3)_2$), 109.3 (s, $C(CH_3)_2$), 109.6 (s, $C(CH_3)_2$). HRMS: *m*/*z* 507.2665, calculated for $C_{23}H_{41}NO_{11}$: 507.2680.

2.3.2. Synthesis of the Ru(II) complexes

*2.3.2.1. [$RuCl_2$(Glun-N,O)$_2$] Na_2 (**I**).* In a Schlenk flask, [$RuCl_2$(DMSO)$_4$] (484.5 mg, 1 mmol) was dissolved in 25 mL of dried ethanol and gently refluxed for 2 h. Then a solution of glucosaminic acid sodium salt (434 mg, 2 mmol) dissolved in 10 mL of ethanol was added and the mixture was heated under reflux for four days. The color of the solution changed from brown-green to brown. The product precipitated from the solution after five days of isothermal evaporation of the solvent in air. The product was filtered out and washed with diethyl ether. The complex was recrystallized from ethanol and dried in a vacuum over P_4O_{10}. Yield: 63%. (*Anal.* Calc. for $C_{12}H_{24}Cl_2N_2Na_2O_{12}Ru$ (M_r = 606.3) C, 23.77; H, 3.99; N, 4.62; Cl, 11.70. Found: C, 23.91; H, 4.15; N, 4.69; Cl, 11.83%). Selected IR bands (KBr, cm^{-1}) (s = strong, m = medium, and w = weak): 3372 (m, ν_{OH}), 3239 (w, ν_{NH}), 1656 (s, $\nu_{C=O}$), 404 (m, ν_{RuO}), 314 (s, ν_{RuCl}), 520 (ν_{RuN}) [34]. ^1H NMR (δ ppm, 300 MHz, D_2O): 3.95 (m, 1H, H-2), 4.32 (m, 1H, H-3), 3.75 (m, 1H, H-4), 3.70 (m, 1H, H-5), 3.63 (m, 2H, H-6).

*2.3.2.2. [$RuCl_2$(1-Tglu)(EtOH)$_2$]Na (**II**).* In a Schlenk flask, [$RuCl_2$(DMSO)$_4$] (484.5 mg, 1 mmol) was dissolved in 25 mL of dried ethanol and gently refluxed for 30 min. Afterwards, 1-thio-β-D-glucose sodium salt (654.6 mg, 3 mmol) dissolved in 20 mL of ethanol was added in one portion. The solution was refluxed for two days and its color changed from orange to black. A brown-black precipitate appeared in the solution after a few days of isothermal evaporation of the solvent in air. The product was filtered out and washed with diethyl ether. The complex was recrystallized from ethanol and dried in a vacuum over P_4O_{10}. Yield: 63%. (*Anal.* Calc. for $C_{10}H_{23}Cl_2NaO_7RuS$ (M_r = 482.3) C, 24.90; H, 4.81; S, 6.65; Cl, 14.70. Found: C, 24.56; H, 4.87; S, 6.78; Cl, 15.35%). Selected IR bands (KBr, cm^{-1}): 3400 (m, ν_{OH}), 422 (w, ν_{RuS}), 325 (s, ν_{RuCl}). ^1H NMR (δ ppm, 300 MHz, D_2O/EtOH-d6): 3.27 (m overlapped, 3H, H-3 + 2H-6), 3.32 (m, 1H, H-4), 3.45 (m, 2H, H-2 + H-5), 4.70 (d, *J* = 8.5 Hz, 1H, H-1).

*2.3.2.3. [Ru_2(EtOH)$_6$(AL)Cl_4] (**III**).* A 100 mL Schlenk flask equipped with a reflux condenser was charged with 40 mL of dried ethanol and [$RuCl_2$(DMSO)$_4$] (484.5 mg, 1 mmol). A freshly prepared solution of the 6′-aminolactose precursor **c** (1.523 g, 3.0 mmol) was added and the resulting mixture was refluxed for five days. The hot solution produced a brown solid which was separated by filtration, washed several times with cold diethyl ether and dried in a vacuum. Yield: 55%. (*Anal.* Calc. for $C_{24}H_{59}Cl_4NO_{16}Ru_2$ (M_r = 961.7) C, 29.97; H, 6.18; N, 1.46; Cl, 14.75. Found: C, 29.52; H, 6.01; N, 1.51; Cl, 15.07%). Selected IR bands (KBr, cm^{-1}): 3383 (s, ν_{OH}); 2894 (w, ν_{NH}); 1151 (m, ν_{CN}); 1055 (m, ν_{C-O}); 540 (w, ν_{RuN}); 458 (m, ν_{RuO}); 3134 (s, ν_{RuCl}). ^1H NMR (δ ppm, 300 MHz, DMSO-d6) (see Section 3).

2.4. Cytotoxicity tests

2.4.1. Cell cultures

The A375 melanoma cell line is a highly invasive cell line from a solid metastatic tumor (ATCC-CRL-1619) [35]. Cells were cultured in RPMI supplemented with 10% FCS and 1% penicillin–streptomycin (10 000 U/ml and 10 000 μg/ml, respectively) in 5% CO_2 at 37 °C. The cell viability was determined by the trypan-blue exclusion dye test, the most common stain used to distinguish viable cells from non-viable cells. In brief, cells were seeded into 12-well plates at 1.5 × 10^5 cells/well in 1.5 mL of growth medium. Cultures were incubated for 24 h, after which the appropriate concentrations of the test substances were added. [$RuCl_2$(DMSO)$_4$] and the

ligands were used at 10^{-4}, 10^{-5} and 10^{-6} M. Adherent and non-adherent cells were pooled after 24, 48 and 72 h treatment and a small sample of each cell suspension was diluted 1:1 in trypan blue and counted under normal light microscopy. The effects of the treatment were quantified as the percentage of cell growth using untreated cells as a control.

2.4.2. Invasivity cells test

About 3×10^6 cells were inoculated into a p/100 plate and left to grow for 24 h. Afterwards, the cell layer was scraped and a 10^{-4} M solution of compound **II** was added to the plate. The number of cells that reached the scraped area were counted after 24, 48 and 72 h in the treated and untreated plates.

3. Results and discussion

Glucosaminic acid was deprotonated by treatment with 1 eq. of NaOH in ethanolic solution to give its sodium salt **a** (Fig. 1), then $[RuCl_2(DMSO)_4]$ was added and the resulting solution was refluxed for 4 days, after which time the color changed from dark-green to brown. Complex **I** (Fig. 2) precipitated as a brown solid upon cooling and concentrating the solution.

Complex **II** (Fig. 2) was prepared by mixing 3 eq. of commercial 1-thio-β-D-glucose sodium salt **b** with 1 eq. of $[RuCl_2(DMSO)_4]$ and refluxing the solution for 2 days. The color changed from orange to brown and a solid precipitated from the concentrated cooled solution.

The ligand **c** was synthesized by the following procedure: β-lactose was transformed to the known O-protected derivative **c′** by the two steps-one pot procedure developed by Barili et al. [36]. Then this compound was converted under Mitsunobu conditions, by phthalimide, diisopropyl azodicarboxylate (DIAD) and triphenylphosphine (TPP), to give the 6′-phtalimidoderivative, **c″**, in a 55% yield (Scheme 1). It is worth noting that this transformation is quite regioselective as the C-2 hydroxy function remains unaffected, likely due to the high steric hindrance at this position. The compound **c″** was in turn converted to the 6′-aminogalacto derivative **c** by treatment with hydrazine in a reasonable yield of 67%. It must be emphasized that the isolation and work-up procedures for compound **c** (see Section 2) are crucial in order to obtain a satisfactory reaction yield. Double sequential treatment with aqueous acid and base to remove acid- and alkali-soluble impurities is necessary. The application of the standard protocol consisting of organic/aqueous phases partitioning could involve significant loses of product and the lack of reproducibility of the final yield. This is probably caused by the amphipolar nature of the aminoalcohol **c**.

The compound **c**, the precursor of the 6′-aminolactose, was reacted with $[RuCl_2(DMSO)_4]$, in boiling ethanol. The complex **III** (Fig. 2) was obtained as a brown precipitate.

Elemental analysis and ESI-MS confirmed the formation of complexes **I–III** with a definite stoichiometry. The analysis of the higher mass region of the mass spectra did not show any signal attributable to the presence of oligomers in the sample. The metal/organic ligand ratios observed are: 1:2 for the complex **I**, 1:1 for the complex **II** and 2:1 for the complex **III** (i.e. a bimetallic species). A significant reduction in the carbon content of complex **III** with respect to the free ligand **c** led us to suspect a deep structural modification of the organic ligand before coordination (see below).

3.1. IR spectra

The infrared spectra of complexes **I–III** show the following bands in the region attributable to ruthenium-ligand bonds (only unambiguous assignments are reported): the spectra of complexes **I** and **III** show the ν(Ru–N) stretching at 520 and 540 cm^{-1}, respectively, while the ν(Ru–O) stretching for compounds **I** and **II** appears at 404 and 458 cm^{-1}, respectively [37–39]. The expected absorption for the Ru–S bond in the spectrum of complex **II** is found at 422 cm^{-1}. Finally, the Ru–Cl stretching vibrations of the three complexes give signals at around 300 cm^{-1} [40,41].

3.2. ^1H NMR

In the ^1H NMR spectra of the complexes **I** and **II**, the signals of the ligands do not show major chemical shift variations with respect to their free form, indicating the lack of any Ru(II) to Ru(III) oxidation process. With regards to complex **III**, a chemical transformation of the free ligand **c** before coordination occurs, as will be discussed in detail later.

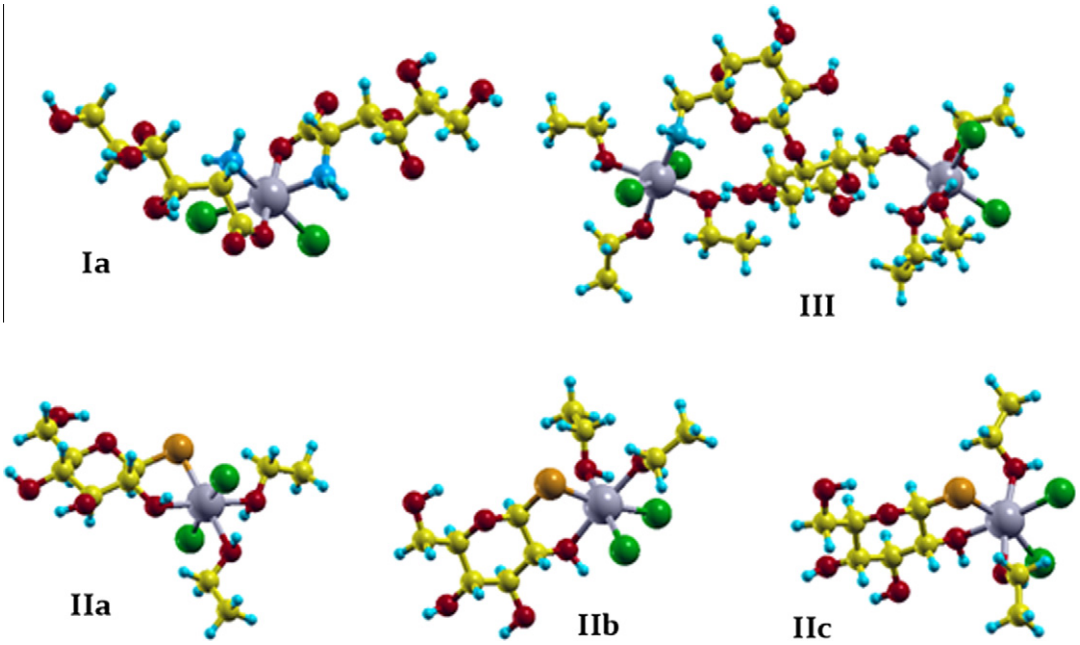

Fig. 2. Proposed structures for the complexes **I–III**.

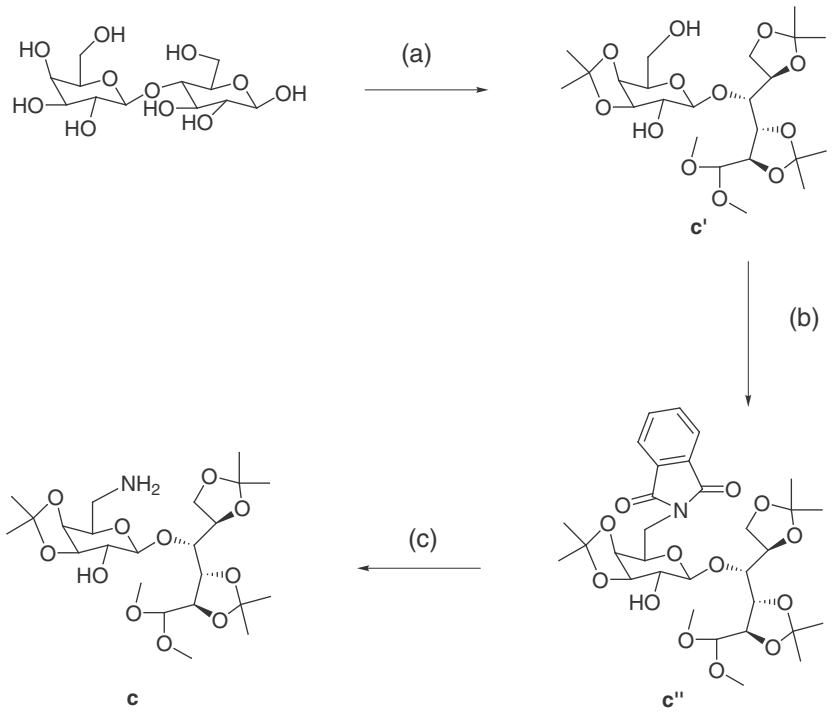

Scheme 1. Synthesis of the ligand **c**. Reagents and conditions: (a) DMP/PTSA (cat.), MeOH, 80 °C; (b) Phtalimide, TPP, DIAD, THF, 0 °C; (c) NH_2NH_2, EtOH, 25 °C.

For complex **I**, a sensible chemical shift variation in the signals of the sugar moiety, concerning in particular protons H-2 and H-3, seems to confirm a coordination mode (Fig. 2) in which the organic ligand is bound *via* its N atom and the negatively charged carboxylate. The proton ^{1}H NMR spectrum of complex **II** also shows signals corresponding to the sugar moiety with chemical shift variations due to coordination. However, a fast exchange due to the solvent employed (D_2O/EtOH-d6) prevent the observation of proton signals of the coordinated ethanol. On the other hand, the presence of two molecules of ethanol is supported by the ESI-MS and elemental analysis data.

The ^{1}H NMR spectrum of complex **III** is worthy of further comment. It shows a group of overlapping signals in the oxygenated proton region (3.30–3.90 ppm) and distinct signals assignable to the CH_2NH_2 moiety (3.10 ppm) and the two peaks corresponding to the acetylic protons of the sugar (4.32 and 4.72 ppm). It is worth noting the disappearance of the isopropilidenic signals; both the NMR data and the M_r obtained from the MS and the elemental analysis show that the complete deprotection of the sugar occurs. This fact can be explained on the ground of the well known Lewis acid character of ruthenium and the nucleophilicity of the solvent that synergistically promote the acetal opening process displayed in Fig. 3. Hence the actual ligand in complex **III** is a molecule of 6′-aminolactose, formed *in situ* from compound **c**.

A group of four methyl signals (Fig. 4) from the coordinated ethanol molecules appears in the aliphatic region of the ^{1}H NMR spectrum; six signals are not distinguishable because they are overlapping, while six peaks in the 3.2–3.8 ppm interval of the COSY spectrum, two of which are overlapped but still distinguishable, are very indicative of the presence of the six diastereotopic coordinated alcohols in the structure proposed for complex **III**.

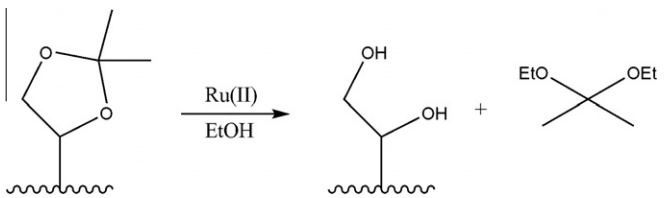

Fig. 3. Acetal opening process.

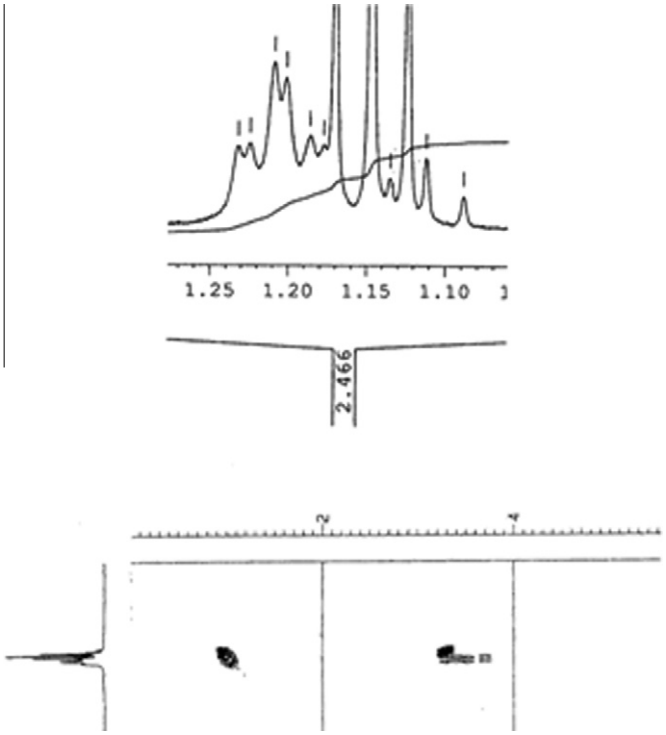

Fig. 4. Details of the ^{1}H NMR and ^{1}H–^{1}H COSY spectra of complex **III**.

3.3. EXAFS investigation

The lack of X-ray crystallographic data due to the non-crystalline nature of the obtained solids does not allow the assignment

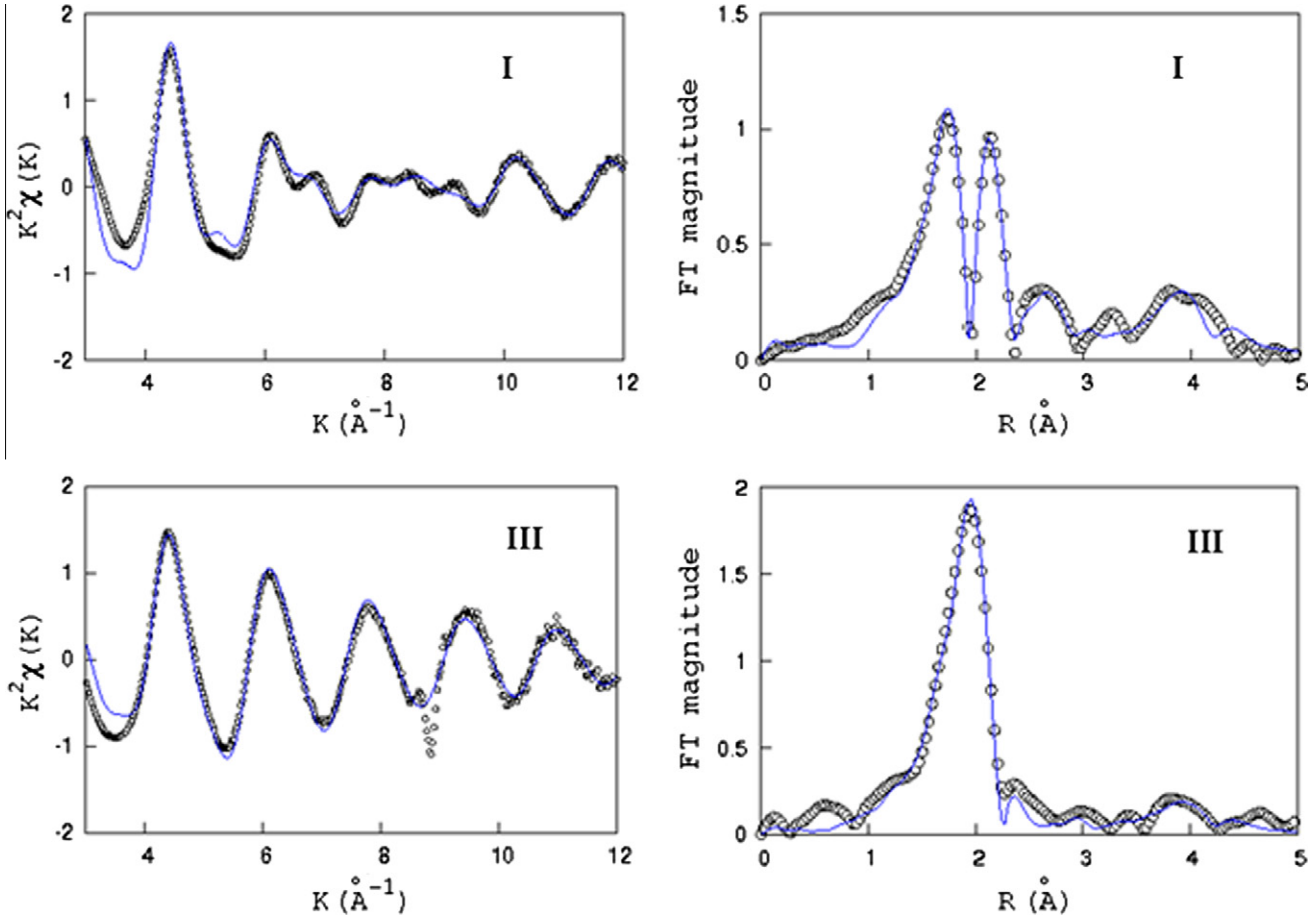

Fig. 5. Experimental (circle) and calculated (solid line) EXAFS functions and their corresponding Fourier transform plots for the different ruthenium(II) complexes measured at the Ru K-edge.

Table 1
EXAFS determined structural parameters at the Ru K-edge.

Complex	A-Bs[a]	N[b]	r[c] (Å)	σ[d] (Å)	E_F[e]
I	Ru–O/N	4	2.16(2)	0.003(1)	4.68
	Ru–Cl	2	2.46(2)	0.003(2)	
	Ru–O–O_{short}	4	3.26(3)	0.003(1)	
	Ru–O–O_{long}	21	4.56(5)	0.008(3)	
III	Ru–O/Cl/N	6	2.39(3)	0.014(3)	4.01
	Ru–Cl–Cl	12	4.60(2)	0.007(1)	

[a] Absorber (A) – backscatters (Bs).
[b] Coordination number.
[c] Interatomic distance.
[d] Debye–Waller factor r with its calculated deviation.
[e] Fermi energy.

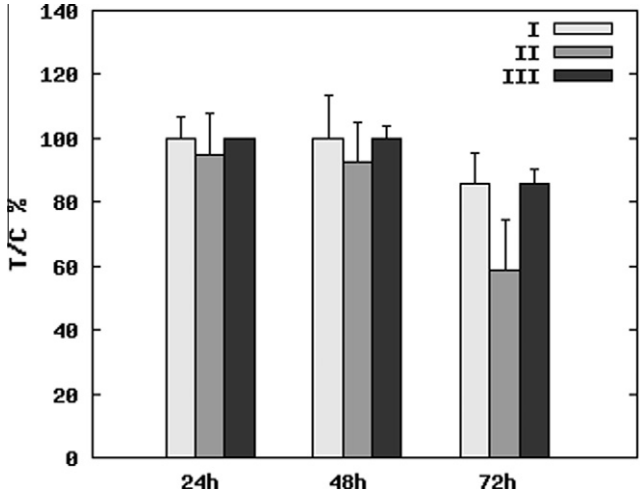

Fig. 6. Treated/control A375 cells growth with 10^{-4} M solutions of complexes **I–III**.

of the exact tridimensional structure of the complexes, such as the exact octahedral environment (i.e. *mer* or *fac*, *cis* or *trans*), and the conformation of the sugar ligand. Attempts of chemical derivatization of the sugar ligands in form of acetates and benzyl ethers with the purpose of obtaining crystalline compounds failed. This could be the consequence of the Lewis acid character of the ruthenium chloride that implies breakage of both the ether and the ester linkages, as one could have been anticipated considering the fate of the precursor **c**. However, the local structure and the coordination geometry of complexes **I** and **III** were determined by extended X-ray absorption fine structure (EXAFS) spectroscopy.

EXAFS spectroscopy provides information on the coordination number, the nature of the scattering atoms surrounding the absorbing atom, the interatomic distances between the absorbing atom and the backscattering atoms and the Debye–Waller factor, which accounts for disorders due to static displacements and thermal vibrations [42,43]. In the fitting procedure, the coordination numbers are held fixed for different backscatterers surrounding the excited atom, and the other parameters, i.e. the interatomic distances, the Debye–Waller factor and the Fermi energy value,

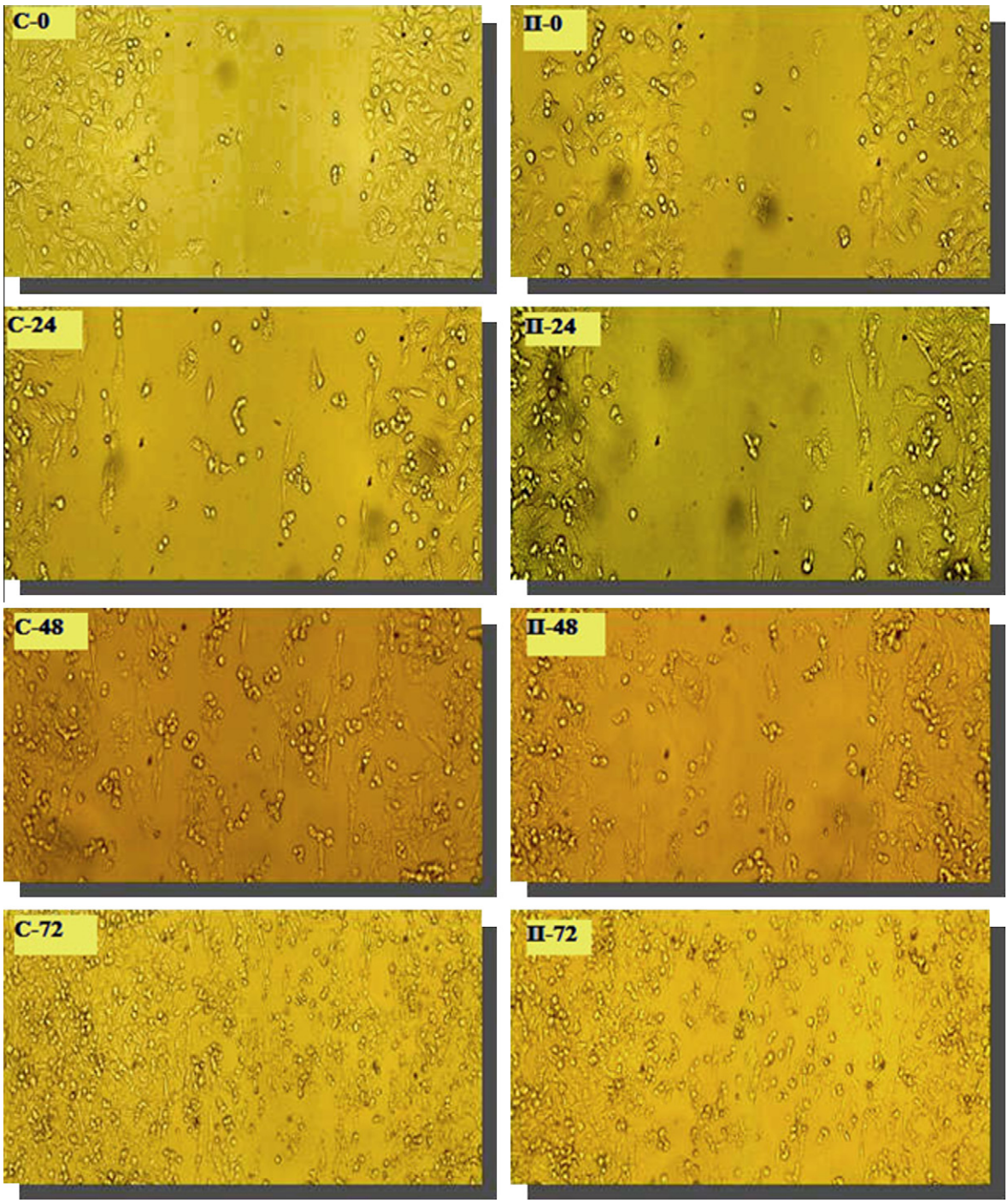

Fig. 7. A375 cells vitality test with a 10^{-4} M solution of complex **II**.

are varied by iteration. The experimental and calculated EXAFS functions in k-space and their Fourier transforms for the ruthenium complexes measured at the Ru–K edge are shown in Fig. 5. The corresponding structural parameters derived from the fit are collected in Table 1. In the analysis of the complex $[RuCl_2(Glun\text{-}N,O)_2]Na_2$, **I**, the first shell consisting of nitrogen and oxygen backscatterers from the coordinating ligands are fitted with a coordination number of four at about 2.16 Å. Owing to the similar backscattering behavior of the neighbors occurring at nearly the same distance, a separate fit of N and O shells cannot be performed, so a single shell model is used with nitrogen amplitude and phase functions. The observed ruthenium–nitrogen and ruthenium–oxygen distances are in agreement with those of analogue ruthenium complexes reported in the literature [44,45]. A second shell is determined at about 2.45 Å and consists of two chlorine atoms [46]; additionally, two shells attributable to oxygen backscatterers are found at 3.26 and 4.56 Å. As regards to the neutral complex $[Ru_2(EtOH)_6(AL)Cl_4]$, **III**, a fit of the first shell at 2.39 Å is possible only if a coordination number of six (N/O/Cl backscatterers) is considered. This problem could originate from the sterically congested environment of the metal centers in complex **III**, which could involve variations of the interatomic distances such that distinct coordination shells for N/O and Cl backscatterers cannot be determined. This would be mirrored in the high value of the Debye–

Waller factor (0.014), witnessing a certain degree of disorder around the ruthenium atoms. A second shell attributed to chlorine backscatterers is determined at 4.60 Å. The EXAFS results are in agreement with 6-fold coordination geometries around the ruthenium atoms in the compounds **I** and **III**.

3.4. Computational results

According to the results of the DFT calculations in the isolated state, the geometries of the most stable isomers of compounds **I**–**III** are reported in Fig. 2. These calculations focused only on the coordination around the ruthenium atom, neglecting the occurrence of different conformations of the ligand molecules. The compound $[RuCl_2(Glun\text{-}N,O)_2]^{2-}$ (**Ia**) has an isomer which is clearly preferred to others: in its coordination geometry the chlorine atoms are *trans* with respect to the aminic nitrogen atoms and *cis* to each other. Within 20 kJ/mol there are two other isomers: the first, where two ligands coordinate symmetrically on the equatorial plane leaving two axial chlorine atoms, is 7 kJ/mol higher in energy, while the second, which shows the chlorine atoms *trans* to the oxygen atoms and *cis* to each other, has an energy value 17 kJ/mol higher. The other two isomers have much higher energy. Calculated vibrational frequencies for the isomer **Ia** are: ν_{RuCl} at 212 and 245 cm^{-1}, ν_{RuO} at 364 cm^{-1} and ν_{RuN} at 509 cm^{-1}. In the case of the species $[RuCl_2(1\text{-}Tglu)(EtOH)_2]^-$, the characterization of structural isomers is not so clearly defined: three isomers of the six structures investigated lie within 1.5 kJ/mol. The most stable isomer (**IIa** in Fig. 2) has two EtOH molecules *trans* with respect to the 1-Tglu ligand; in the second isomer (**IIb**, 1.1 kJ/mol higher in energy) the above *trans* positions are occupied by chlorine, and in the third isomer (**IIc**, 1.4 kJ/mol higher) Cl and EtOH are *trans* to the S and O atoms of 1-Tglu, respectively. According to the Boltzmann distribution, in gas phase the population of the three isomers should be 45%, 30% and 25%, respectively. Globally, the representative normal modes of these structures have the following frequency values: ν_{RuCl} in the range 240–280 cm^{-1}, and ν_{RuO} in the range 453–511 cm^{-1}. Seven isomers of compound **III** have been investigated with regards to the coordination of the ligands around the two ruthenium centers. Due to the conformational flexibility of the 6′-aminolactose ligand, small energy differences between structural isomers could be not indicative of a preferred coordination. On the other hand, the only isomers which should have a significant population in the gas phase share the same coordination sphere around the ruthenium atom bound to the aminic moiety of 6′-aminolactose (Ru^I) and slightly differ for the ligands arrangement around the second ruthenium atom, the one coordinated to the –OH group of the disaccharide. In this kind of isomers, where the EtOH ligands around the Ru^I atom are in a *mer* arrangement and the chlorine atoms are *trans* to each other, the ν_{RuCl} stretching frequencies are in the range 243–315 cm^{-1}, ν_{RuO} in the range 341–374 cm^{-1} and ν_{RuN} is at 530 cm^{-1}.

3.5. Biological activity

The cytotoxicity of complexes **I**–**III** was investigated on a A375 cell line target. The cell cultures were incubated with 10^{-4}, 10^{-5} and 10^{-6} M solutions of complexes **I**–**III** and the cell growth was determined with respect to the untreated cells (control). The results obtained with 10^{-4} M are reported in Fig. 6. The other solutions were inactive.

Of the three compounds tested, only complex **II** shows a 50% growth inhibition activity after 72 h, with an extrapolated IC_{50} value of $(5.08 \pm 1.21) \times 10^{-4}$ M. The *in vitro* cytotoxicity of this compound against the A375 cell line is comparable to that reported by Zorzet et al. [47] for NAMI-A against MCF-7, LoVo, KB and TS/A tumor cells in the same range of concentration. These authors also showed a significant inhibition of the invasiveness of the TS/A adenocarcinoma cells *in vitro*, associated with an inhibitory effect – both in the number and in the weight of the outbreaks – toward the metastasis of the Lewis lung carcinoma in mice. The combination of these results was proposed as a pre-requisite for a ruthenium compound to possess a selective anti-metastasis effect *in vivo* [47]. In light of this, we were encouraged to investigate the residual mobility and proliferative capacity of A375 cells after treatment with the active complex **II**. Hence an invasiveness test was performed at 24, 48 and 72 h (Fig. 7). As reported in Fig. 7, cells treated with complex **II** demonstrate a significant reduction in their invasion capacity with respect to the untreated cells. Considering the mechanism of action of the metastasis-inhibiting ruthenium compounds [18,47], the partial inhibition of the cell mobility can be considered as a valuable starting point for further specific biological studies.

4. Conclusions

Two new mononuclear and one binuclear ruthenium(II) complexes were synthesized and structurally characterized by elemental analysis, IR, NMR, ESI-MS, EXAFS and DFT calculations. For complex **I**, the data show the coordination of two molecules of glucosaminic acid sodium salt acting as a bidentate ligand, probably through the aminic and the carboxylate group with an ester type coordination. For complex **II**, a five-membered metallocycle has been postulated in which a strong Ru–S bonds should stabilize the structure. Complex **III** has a more complicated bond pattern that should include two metallic centers with similar environments. Compound **II** exhibits promising biological properties *in vitro*: despite a weak direct cytotoxicity, this complex shows anti-invasive activity against A375 melanoma cell lines. The combination of these observed biological properties should encourage further investigations into the *in vivo* antitumor activity of this compound.

Acknowledgements

Financial supports of Università degli Studi di Palermo are gratefully acknowledged (OIPA078W7F, OIPA0737W2). We thank XAFS beamline scientist, Dr. Luca Olivi, for assistance during data collection. Sincrotrone Elettra, Trieste is gratefully acknowledged for financial support during the campaign of EXAFS measurements. We wish to thank Dr. ssa M. A. Costa and Dr. ssa G. Barbieri of the Istituto di Biomedicina e Immunologia Molecolare "Alberto Monroy", Consiglio Nazionale delle Ricerche (CNR), Palermo, Italy, for their helpful suggestions and support.

References

[1] (a) M.J. Clarke, F. Zhu, D.R. Frasca, Chem. Rev. 99 (1999) 2511;
(b) S.M. Page, S.R. Boss, P.D. Barker, Future Med. Chem. 1 (2009) 541.
[2] M.A. Jakupec, M. Galanski, V.B. Arion, C.G. Hartinger, B.K. Keppler, J. Chem. Soc., Dalton Trans. 2 (2008) 183.
[3] P.C.A. Bruijnincx, P.J. Sadler, Curr. Opin. Chem. Biol. 12 (2008) 197.
[4] L. Ronconi, P.J. Sadler, Coord. Chem. Rev. 251 (2007) 1633.
[5] P.J. Dyson, G. Sava, J. Chem. Soc., Dalton Trans. (2006) 1929.
[6] C.S. Allardyce, A. Dorcier, C. Scolaro, P.J. Dyson, Appl. Organomet. Chem. 19 (2005) 1.
[7] R. Paschke, C. Paetz, T. Mueller, H.J. Schmoll, H. Mueller, E. Sorkau, E. Sinn, Curr. Med. Chem. 10 (2003) 2033.
[8] M. Galanski, V.B. Arion, M.A. Jakupec, B.K. Keppler, Curr. Pharm. Des. 9 (2003) 2078.
[9] C.X. Zhang, S.J. Lippard, Curr. Opin. Cell Biol. 7 (2003) 481.
[10] R.A. Sánchez-Delgado, A. Anzellotti, L. Suárez, Met. Ions Biol. Syst. 41 (2004) 379.
[11] M.J. Clarke, Coord. Chem. Rev. 232 (2002) 69.
[12] (a) G. Sava, I. Capozzi, K. Clerici, G. Gagliardi, E. Alessio, G. Mestroni, Clin. Exp. Metastasis 16 (1998) 371;
(b) G. Sava, K. Clerici, I. Capozzi, Anticancer Drugs 10 (1999) 129;

(c) G. Sava, R. Gagliardi, M. Cocchietto, K. Clerici, I. Capozzi, M. Marrella, E. Alessio, G. Mestroni, R. Milanino, Pathol. Oncol. Res. 4 (1998) 30.
[13] J.M. Rademaker-Lakhai, D. van den Bongard, D. Pluim, J.H. BeiJnen, J.H.M. Schellens, Clin. Cancer Res. 10 (2004) 3717.
[14] M. Groessl, E. Reisner, C.G. Hartinger, R. Eichinger, O. Semenova, A.R. Timerbaev, M.A. Jakupec, V.B. Arion, B.K. Keppler, J. Med. Chem. 50 (2007) 2185.
[15] A. Bergamo, G. Sava, J. Chem. Soc., Dalton Trans. (2007) 1267.
[16] I. Bratsos, S. Jedner, T. Gianferrara, E. Alessio, Chimia 61 (2007) 692.
[17] M.A. Jakupec, V.B. Arion, S. Kapitza, E. Reisner, A. Eichinger, M. Pongratz, B. Marian, N. Graf von Keyserlingk, B.K. Keppler, J. Clin. Pharm. Therap. 43 (2005) 595.
[18] B. Gava, S. Zorzet, P. Spessotto, M. Cocchietto, G. Sava, J. Pharm. Exp. Therap. 317 (2006) 284.
[19] P.J. Dyson, Chimia 61 (2007) 698.
[20] G. Sava, S. Pacor, F. Bregant, V. Ceschia, G. Mestroni, Anti-Cancer Drugs 1 (1990) 99.
[21] G. Sava, S. Pacor, S. Zorzet, E. Alessio, G. Mestroni, Pharm. Res. 21 (1989) 617.
[22] M. Coluccia, G. Sava, F. Loseto, A. Nassi, A. Boccarelli, D. Giordano, E. Alessio, G. Mestroni, Eur. J. Cancer 29 (1993) 1873.
[23] E. Alessio, G. Mestroni, G. Nardin, W.M. Attia, M. Calligaris, G. Sava, S. Zorzet, Inorg. Chem. 27 (1988) 4099.
[24] A.G. Glass, R.N. Hoover, J. Am. Med. Assoc. 262 (1989) 2097.
[25] A. Jemal, A. Thomas, T. Murray, M. Thun, CA Cancer J. Clin. 52 (2002) 23.
[26] D.S. Rigel, Derm. Clin. 20 (2002) 601.
[27] V. Rajendiran, M. Murali, E. Suresh, S. Sinha, K. Somasundaram, M. Palaniandavar, J. Chem. Soc., Dalton Trans. (2008) 148.
[28] (a) C.G. Hartinger, A.A. Nazarov, S.M. Ashraf, P.J. Dyson, B.K. Keppler, Curr. Med. Chem. 15 (2008) 2574;
(b) I. Berger, M. Hanif, A.A. Nazarov, C.G. Hartinger, R.O. John, M.L. Kuznetsov, M. Groessl, F. Schmitt, O. Zava, F. Biba, V.B. Arion, M. Galanski, M.A. Jakupec, L. Juillerat-Jeanneret, P.J. Dyson, B.K. Keppler, Chem. Eur. J. 14 (2008) 9046.
[29] W. Schöniger, Mikrochim. Acta 9 (1955) 123.
[30] B. Ravel, M. Newville, J. Synchrotron Rad. 12 (2005) 537.
[31] J.J. Rehr, J. Mustre de Leon, S.I. Zabinsky, R.C. Albers, J. Am. Chem. Soc. 113 (1991) 5135.
[32] M.J. Frisch, G.W. Trucks, H.B. Schlegel, G.E. Scuseria, M.A. Robb, J.R. Cheeseman, J.A. Montgomery, Jr., T. Vreven, K.N. Kudin, J.C. Burant, J.M. Millam, S.S. Iyengar, J. Tomasi, V. Barone, B. Mennucci, M. Cossi, G. Scalmani, N. Rega, G.A. Petersson, H. Nakatsuji, M. Hada, M. Ehara, K. Toyota, R. Fukuda, J. Hasegawa, M. Ishida, T. Nakajima, Y. Honda, O. Kitao, H. Nakai, M. Klene, X. Li, J.E. Knox, H.P. Hratchian, J.B. Cross, V. Bakken, C. Adamo, J. Jaramillo, R. Gomperts, R.E. Stratmann, O. Yazyev, A.J. Austin, R. Cammi, C. Pomelli, J.W. Ochterski, P.Y. Ayala, K. Morokuma, G.A. Voth, P. Salvador, J.J. Dannenberg, V.G. Zakrzewski, S. Dapprich, A.D. Daniels, M.C. Strain, O. Farkas, D.K. Malick, A.D. Rabuck, K. Raghavachari, J.B. Foresman, J.V. Ortiz, Q. Cui, A.G. Baboul, S. Clifford, J. Cioslowski, B.B. Stefanov, G. Liu, A. Liashenko, P. Piskorz, I. Komaromi, R.L. Martin, D.J. Fox, T. Keith, M.A. Al-Laham, C.Y. Peng, A. Nanayakkara, M. Challacombe, P.M.W. Gill, B. Johnson, W. Chen, M.W. Wong, C. Gonzalez, J.A. Pople, GAUSSIAN 03, Revision D.02, Gaussian, Inc., Wallingford CT, 2004.
[33] P.J. Stephens, J.F. Devlin, C.F. Chabalowsky, M.J. Frisch, J. Phys. Chem. 98 (1994) 11623.
[34] S. Kannan, K.N. Kumar, R. Ramesh, Polyhedron 27 (2008) 701.
[35] D.J. Giard, S.A. Aaronson, G.J. Todaro, J. Natl. Cancer Inst. 51 (1973) 1417.
[36] P.L. Barili, G. Catelani, F. D'Andrea, F. De Rensis, P. Falcini, Carbohydr. Res. 298 (1997) 75.
[37] K. Nakamato, Infrared and Raman Spectra of Inorganic and Coordination Compounds, Wiley Interscience, New York, 1971.
[38] P. Byabartta, P.K. Santra, T.K. Misra, C. Sinha, C.H.L. Kennard, Polyhedron 20 (2001) 905.
[39] S. Goswami, R. Mukherjee, A. Chakravorty, Inorg. Chem. 22 (1983) 2825.
[40] E. Alessio, G. Balducci, M. Calligaris, G. Costa, W.M. Attia, G. Mestroni, Inorg. Chem. 30 (1991) 609.
[41] J. Lewis, F.E. Mabbs, R.A. Walton, J. Am. Chem. Soc. 89 (1967) 1366.
[42] B.K. Teo, EXAFS: Basic Principles and Data Analysis, Springer, Berlin, 1986.
[43] F.W. Lytle, D.E. Sayers, E.A. Stern, Phys. Rev. B 11 (1975) 4825.
[44] J.F. Bickley, A.A. La Pensée, S.J. Higgins, C.A. Stuart, J. Chem. Soc., Dalton Trans. (2003) 4663.
[45] W.L. Man, T.M. Tang, T.W. Wong, T.C. Lau, S.M. Peng, W.T. Wong, J. Am. Chem. Soc. 126 (2004) 478.
[46] P.M.T. Piggot, L.A. Hall, A.J.P. White, D.J. Williams, Inorg. Chim. Acta 357 (2004) 207.
[47] S. Zorzet, A. Bergamo, M. Cocchietto, A. Sorc, B. Gava, E. Alessio, E. Iengo, G. Sava, J. Pharm. Exp. Therap. 295 (2000) 927.